Giorgio Volpi, Claudio Garino, Emanuele Priola, Claudia Barolo

A new auspicious scaffold for small dyes and fluorophores

Dyes and Pigments, 2022, 197, 109849

DOI: 10.1016/j.dyepig.2021.109849

A new auspicious scaffold for small dyes and fluorophores

Giorgio Volpi,[a] Claudio Garino,*[a] Emanuele Priola,[a,b] Claudia Barolo[a,c]

[a] *Dept. of Chemistry and NIS Interdepartmental Centre, University of Turin, Italy*
[b] *CrisDI Center of Crystallography, University of Turin, Italy*
[c] *ICxT Interdepartmental Centre, University of Turin, Italy*

* corresponding author claudio.garino@unito.it

Abstract

An unprecedented chromophore, based on a nitrogen fused tricyclic heterocycle, is presented. This prototype molecule can be considered a "rigidified" monomethine cyanine dye and the central core is isoelectronic to pyridine-based BODIPY analogues, such as boron difluoride dipyridylmethene. The chromophore was synthesized and its photophysical properties examined. The new molecule can be considered the starting point to develop dyes, fluorophores or dual-emission fluorescent probes with excitation window in the green region of the spectrum.

1. Introduction

Since Perkin's accidental discovery of mauve in 1856, synthetic dyes replaced those of natural origin and today only logwood is commercially employed. Considering their scientific and technological applications, it is clear that dyestuffs not only have aesthetic or commercial values and small organic dyes and fluorophores are indeed fundamental tools for biological, medical and chemical research.
Many organic chromophores have been developed and, after a century of chemistry, xanthene, coumarin, resorufin, acridone, cyanine and BODIPY derivatives are commonly employed to stain, label or probe chemical and biological systems.[1–5] Such organic compounds are relatively inexpensive, easy to handle and generally applicable to any sample. Indeed, they endured the advent of fluorescent proteins, quantum dots, luminescent complexes and other platforms.[6–8]
Despite this long history, the structural modification of small organic dyes and fluorophores continues to be an active and stimulating topic. For example, although fluorogenic molecules excited in the ultraviolet, blue, orange and red are well established, there is no general scaffold for molecules excited with green light (~545 nm), leaving this spectral region underutilized in experiments involving fluorogenic compounds.[9] In the last ten years, many efforts have been made to replace the oxygen in the xanthene scaffold with carbon,[9–11] silicon,[12–14] germanium or tin,[15] phosphorus,[16,17] or sulphur,[18] in order to get longer wavelength derivatives.

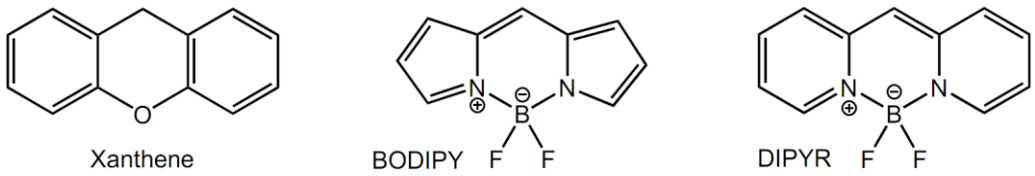

Figure 1. Chemical structure of xanthene, BODIPY and DIPYR.

This paper describes the development of a new heterocyclic scaffold (Fig. 2), consisting in a nitrogen fused tricyclic heterocycle, structurally halfway through xanthenes and BODIPYs. As BODIPYs it can be considered as being a "rigidified" monomethine cyanine dye and the central core is isoelectronic to pyridine-based BODIPY analogues, such as boron difluoride dipyridylmethene (DIPYR, Fig. 1).[19]

2. Results and discussion

The core of this prototype chromophore consists of a zwitterionic structure derived from the 6H-dipyrido[1,2-c:2',1'-f]pyrimidin-5-ium, with a negative charged oxygen balancing the charge of the pyrimidinium moiety. Depending on the pH of the medium, the molecule is present in the acid form **1** (zwitterionic imidic acid in solution and amide tautomer in the solid state) or in the base form **2**. To the best of our knowledge, this scaffold has never been reported before. The closer reference in the literature is the structure hypothesised by G. Scheibe and co-workers in 1961 for a red dye, named "*pyridinrot*" (pyridine red) by analogy with quinoline red derivatives.[20,21]

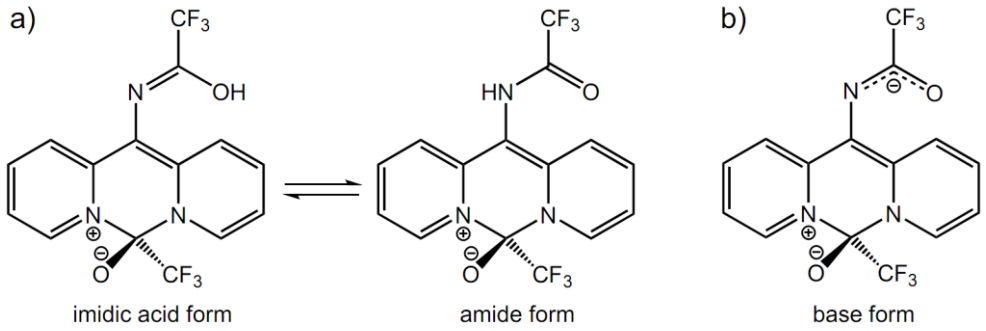

Figure 2. Chemical structure of **1** (imidic acid and amide tautomers) and of its conjugate base **2**.

Compound **1** was synthesized reacting bis(pyridin-2-yl)methanamine with trifluoroacetic anhydride in presence of pyridine, in a dichloromethane solution at –15 °C, scheme 1 (see supplementary material for details). These reaction conditions also lead to the formation of a 14% of 1-(pyridin-2-yl)-3-(trifluoromethyl)imidazo[1,5-*a*]pyridine side-product. Indeed, the pyridin-2-ylmethanamine skeleton is generally employed in analogous conditions to obtain a different cyclization (see scheme SI1)[22] and, actually, pyridin-2-ylmethanamine derivatives have been widely employed in different conditions to obtain several imidazo[1,5-*a*]pyridines in high yields.[23–26] On the other hand, bis(pyridin-2-yl)methanamine in the current reaction conditions mainly leads to this completely new cyclization, never reported before.

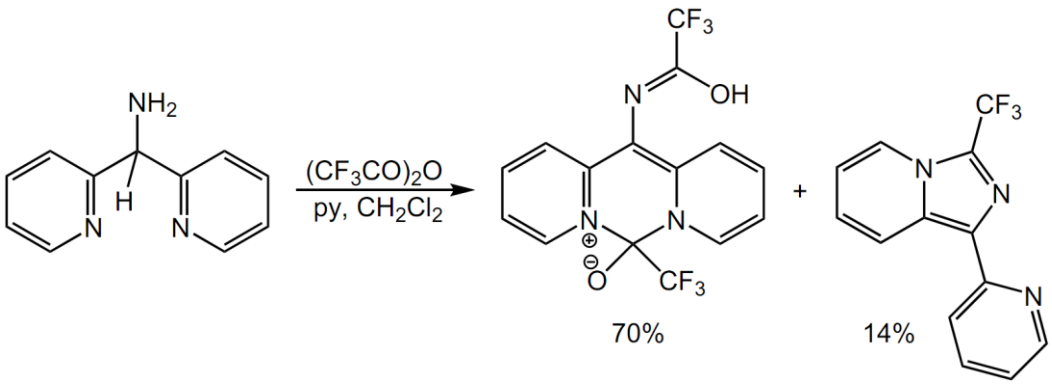

Scheme 1. Synthesis of **1**.

Compound **1** was obtained as an orange powder, in high yield. High resolution mass spectrometry, infrared (Fig. S3) and ^{1}H- ^{13}C- ^{19}F-NMR spectroscopies (Fig. 3, ^{1}H NMR of **1** and **2**, and supplementary material Fig. S1) are consistent with the proposed structures.

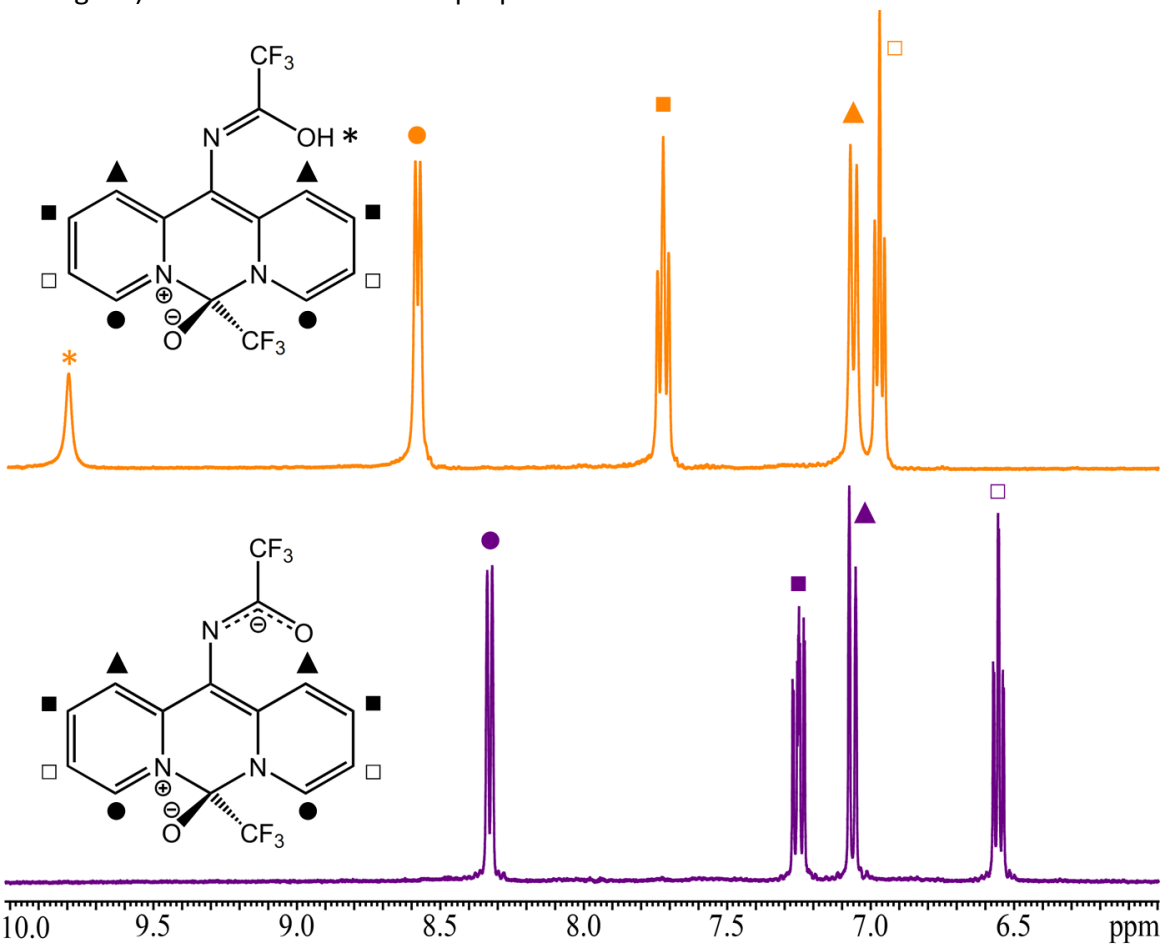

Figure 3. ^{1}H-NMR spectra of **1** (orange) and **2** (violet) in acetone-d6 solution.

The molecular structure of **1** (Fig. 4) was solved by single crystal x-ray diffraction on red prismatic crystals obtained by slow evaporation of a dichloromethane solution of **1**. The molecule crystallizes in the non-centrosimmetric orthorhombic space group $Cmc2_1$. The crystallization of achiral molecules in non-centrosymmetric space group is a rare phenomenon, especially in the case of rigid molecules.[27] The polarity of the structure has been reliably assigned through Cu-Kα radiation diffraction measurement on the same crystal. The presence of a fraction of merohedral twinning, due to the energetic similarity of the two conformations, has been detected. The asymmetric unit (Fig. 4b) is doubled by the central mirror plane present in the molecular point group of the solidified configuration, indicating the molecule is achiral.

The obtained molecular structure is quite unusual and displays a sp^3 hybridized carbon (C2) embedded in a polycyclic aromatic system. Indeed, the careful analysis of the geometry demonstrates the partial, but relevant, delocalization of the double bonds along the three rings. Similarly to the boron atom of BODIPY, the C2 carbon atom is bound to two nitrogen of the heterocyclic aromatic system, while the other two positions are occupied by a $–CF_3$ and an alcoholate group. From a thorough search in literature and on crystallographic databases we have not found anything similar.

Looking in detail, the three rings in the molecular structure (Fig. 4a) are not perfectly coplanar: the angle between the centroids of the two lateral rings respect to the centroid of the central ring is 160.5(7)°, defining a bended scaffold. At the same time, the central ring adopts the boat conformation, with a distortion from planarity of 28.5(7)° on the C2 vertex and of 12.3(7)° on the C8 vertex. However, the bond distances around the C8 ($d_{C8–C7} = d_{C8–C7'}$ = 1.394(3) Å) are shorter than an average single carbon-carbon bond and together with the almost planar geometry confirm that this fragment connects the two lateral aromatic rings by delocalizing double bonds. On the other hand, C2 presents a slightly distorted tetrahedral geometry ($ang_{N1–C2–N1'}$ = 104.7(2)° and $ang_{O1–C2–N1}$ = 114.01(17)°), and the surrounding ring distances confirm its separation from the aromatic system ($d_{C2–N1} = d_{C2–N1'}$ = 1.531(3) Å). At the same time, the C2–O1 distance is consistent with a single bond ($d_{C2–O1}$ = 1.274(4) Å) and with the presence of a charged alcoholate group (complete absence of residual electron density characteristic of an alcoholic hydrogen). In the case of the C9–O2 bond, the shorter distance ($d_{C9–O2}$ = 1.206(4) Å) is consistent with the double bonded carbonyl of the amidic group (see Fig. S2 in the supplementary material for the comparison with the distance distribution in the CSD database), that is reflected in the vibrational spectra of the solid sample by the C=O stretching at 1730 cm^{-1} and by the N–H stretching at 3100 cm^{-1} (Fig. S3). This characteristic, together with the C8–N2 distance of 1.426(4) Å, confirms the presence of the amide tautomer in the solid state, respect to the imidic acid form present in solution (C=N stretching at 1750 cm^{-1} and O–H stretching at 3390 cm^{-1}, Fig. S3). This fact is quite common and can be attributed to the packing forces. In the crystal, the amidic and the alcoholate groups are involved in the formation of hydrogen bonded chains along the c-axis (Fig. 4c), further confirming the position of the tautomeric hydrogen.

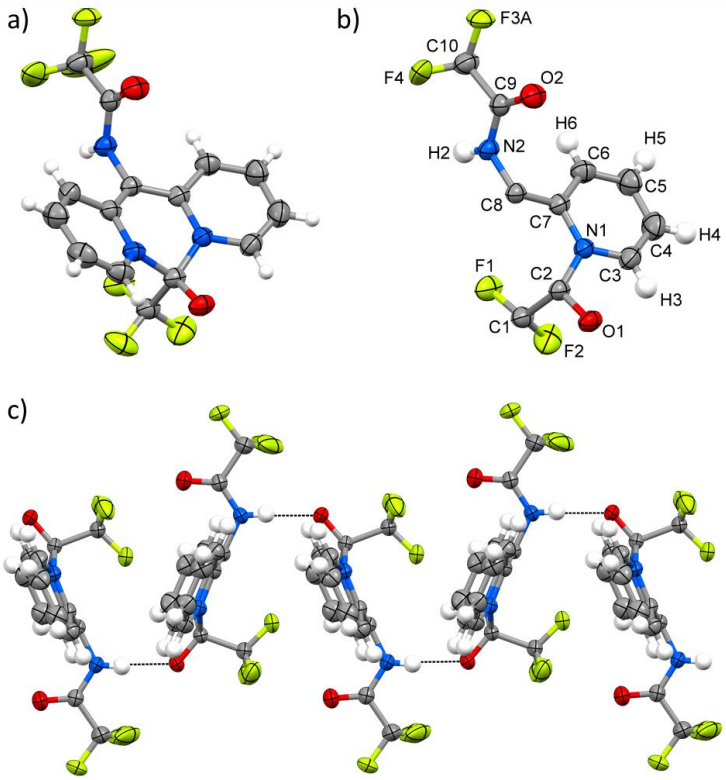

Figure 4. a) X-ray structure of **1** (amide tautomer) with displacement ellipsoids drawn at 50% probability, b) asymmetric unit with atom labels and numeration followed in the text, c) hydrogen bonded chain of molecules along the c-axis.

The optical characterization of the new scaffold was carried out in aqueous solution. The UV-vis electronic absorption and emission spectra of **1** and **2** are reported in Fig 5. The main absorption band of **1** falls in the blue region of the spectrum (at 500 nm). When the pH changes from 9.0 to 11.0, the orange solution of **1** turns violet (see inset Fig. 5). The corresponding UV–vis spectrum of **2** is characterized by an intense absorption in the green region of the spectrum (at 560 nm), highlighting a bathochromic-shift of about 60 nm of the low energy absorption band upon deprotonation of **1** to form **2**. Meanwhile, the green fluorescence emission of **1**, centred at 540 nm, disappears in favour of the new emission peak of **2**, in the red region of the spectrum (630 nm). The emission quantum yield and lifetime of this prototype (ϕ 1% and τ = 3 ns for **1**, lower for **2**) are limited and could be improved by appropriate modification to alter properties and function, as successfully achieved for all the fluorophore classes currently in use.[6,28] The double emission (in the green region for **1** and in the red region of the spectrum for **2**), together with the excitation windows of **2** in the green, a spectral region chronically underutilized due to the lack of commercial fluorophores, make this new scaffold extremely promising.

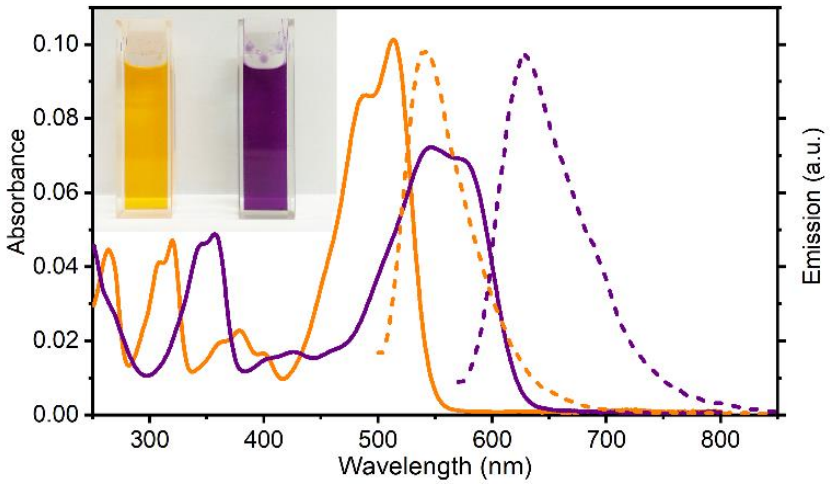

Fig. 5 UV–vis absorption (solid lines) and emission (dashed lines) spectra of **1** (orange, pH 9.0) and **2** (violet, pH 11.0) in aqueous solution. Insert: image of the solutions of **1** and **2**.

The spectrophotometric determination of the equilibrium constant (Fig 6) provided a value of pKa = 9.98. At physiological pH the molecule is present in the zwitterionic form, a fundamental characteristic for cell membrane permeability.

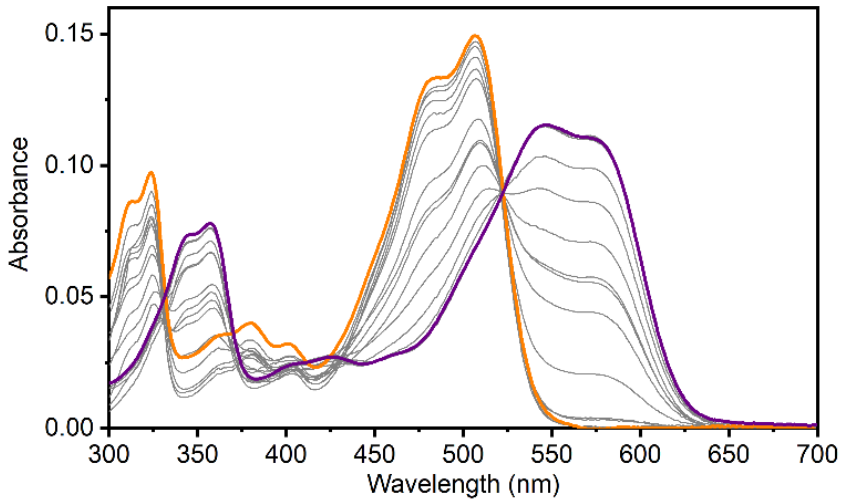

Fig. 6 Absorbance curves for acidic (pH 2, orange curve), basic (pH 14, violet curve), and intermediate pH (grey curves) solutions.

DFT and TDDFT calculations, performed to gain insights into the structural and electronic properties of **1** and **2**, are in perfect agreement with the experimental results (B3LYP/6-311G**/PCM level of theory, see computational section of the supplementary material for more details). In particular, the comparison of experimental and calculated absorption spectra (Fig. 7) displays a very good match, allowing to characterize the main absorption feature of both **1** and **2** as originating from a π-π* electronic transition (see Fig. S4) involving the depopulation of the HOMO and the population of the LUMO. The bathochromic shift of the low energy absorption band upon deprotonation is accurately reproduced by TDDFT calculations (0.27 eV for both experimental and calculated values), and can be ascribed to an energy increase of the HOMO of **2**, if compared to **1**.

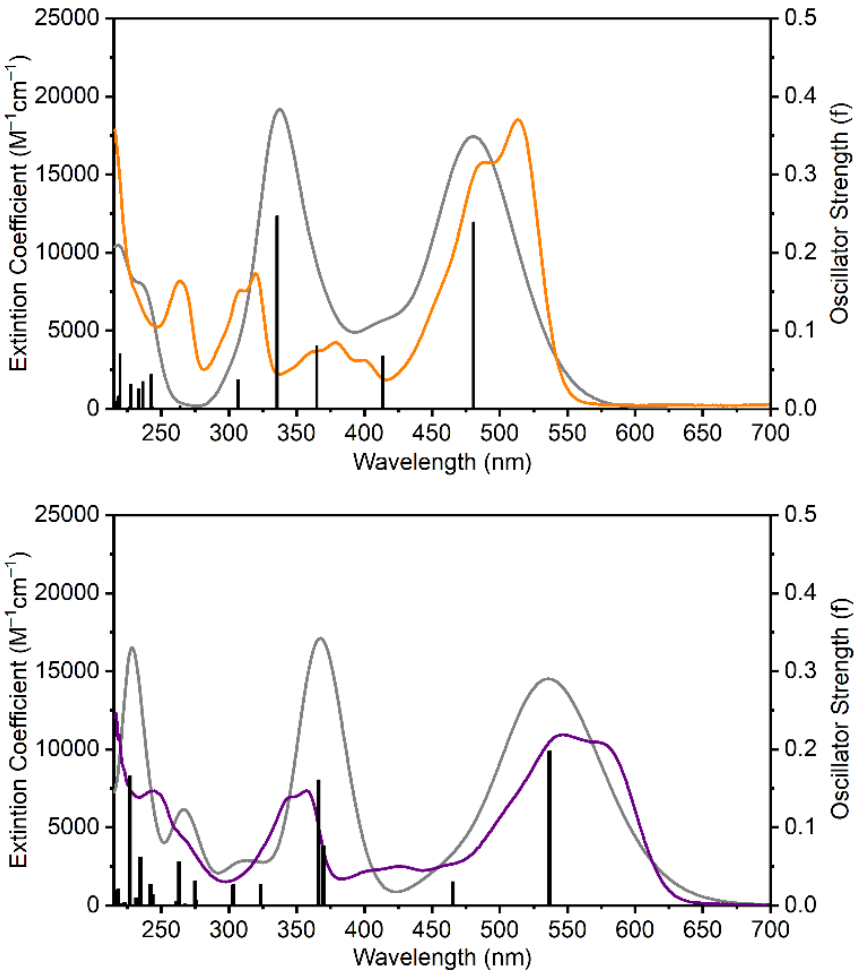

Fig. 7 Experimental electronic absorption spectra of **1** (top, orange curve, pH 2) and **2** (bottom, violet curve, pH 14) in aqueous solutions together with calculated singlet excited state transitions (vertical bars with height equal to the oscillator strength (f) values).

3. Conclusions

In conclusion, we report here an unprecedented molecular scaffold suitable to develop new small dyes. The proposed zwitterionic structure is water soluble, stable in a large pH range and can be obtained in a simple and economical way, through a single synthetic step that does not require organometallic reagents, unlike replacing the ether functionality of the xanthene ring. Furthermore, the unprecedented X-ray structure obtained for the amide tautomer of **1** could clarify a number of molecules obtained in the past, such as the "*pyridinrot*", whose structure in fact remained unknown.

The optical properties of the neutral form (**1**) and its conjugated base (**2**) are extremely promising. The scaffold can be considered the starting point to develop dyes, fluorophores or dual-emission ratiometric fluorescent probes for analytical sensing and optical imaging. In particular, the excitation windows of the base form, in the green region of the spectrum, covers a spectral region chronically underutilized in experiments involving fluorogenic compounds, due to the lack of fluorophores. At the current stage, the low emission quantum yield and the short lifetime could be improved, although this is not so critical for ratiometric fluorescence probes with two reversible signal changes. Future synthetic efforts are planned in our laboratories to obtain superior structural analogues.

References

[1] Wysocki LM, Lavis LD. Advances in the chemistry of small molecule fluorescent probes. Curr Opin Chem Biol 2011;15:752–9. https://doi.org/10.1016/j.cbpa.2011.10.013.

[2] Terai T, Nagano T. Small-molecule fluorophores and fluorescent probes for bioimaging. Pflüg Arch - Eur J Physiol 2013;465:347–59. https://doi.org/10.1007/s00424-013-1234-z.

[3] Hamilton GRC, Sahoo SK, Kamila S, Singh N, Kaur N, Hyland BW, et al. Optical probes for the detection of protons, and alkali and alkaline earth metal cations. Chem Soc Rev 2015;44:4415–32. https://doi.org/10.1039/C4CS00365A.

[4] Fu Y, Finney NS. Small-molecule fluorescent probes and their design. RSC Adv 2018;8:29051–61. https://doi.org/10.1039/C8RA02297F.

[5] Sun X, Liu T, Sun J, Wang X. Synthesis and application of coumarin fluorescence probes. RSC Adv 2020;10:10826–47. https://doi.org/10.1039/C9RA10290F.

[6] Lavis LD. Teaching Old Dyes New Tricks: Biological Probes Built from Fluoresceins and Rhodamines. Annu Rev Biochem 2017;86:825–43. https://doi.org/10.1146/annurev-biochem-061516-044839.

[7] Specht EA, Braselmann E, Palmer AE. A Critical and Comparative Review of Fluorescent Tools for Live-Cell Imaging. Annu Rev Physiol 2017;79:93–117. https://doi.org/10.1146/annurev-physiol-022516-034055.

[8] Lavis LD, Raines RT. Bright Ideas for Chemical Biology. ACS Chem Biol 2008;3:142–55. https://doi.org/10.1021/cb700248m.

[9] Grimm JB, Sung AJ, Legant WR, Hulamm P, Matlosz SM, Betzig E, et al. Carbofluoresceins and Carborhodamines as Scaffolds for High-Contrast Fluorogenic Probes. ACS Chem Biol 2013;8:1303–10. https://doi.org/10.1021/cb4000822.

[10] Arden-Jacob J, Frantzeskos J, Kemnitzer NU, Zilles A, Drexhage KH. New fluorescent markers for the red region. Spectrochim Acta A Mol Biomol Spectrosc 2001;57:2271–83. https://doi.org/10.1016/S1386-1425(01)00476-0.

[11] Kolmakov K, Belov VN, Wurm CA, Harke B, Leutenegger M, Eggeling C, et al. A Versatile Route to Red-Emitting Carbopyronine Dyes for Optical Microscopy and Nanoscopy. Eur J Org Chem 2010;2010:3593–610. https://doi.org/10.1002/ejoc.201000343.

[12] Egawa T, Koide Y, Hanaoka K, Komatsu T, Terai T, Nagano T. Development of a fluorescein analogue, TokyoMagenta, as a novel scaffold for fluorescence probes in red region. Chem Commun 2011;47:4162–4. https://doi.org/10.1039/C1CC00078K.

[13] Kushida Y, Nagano T, Hanaoka K. Silicon-substituted xanthene dyes and their applications in bioimaging. Analyst 2015;140:685–95. https://doi.org/10.1039/C4AN01172D.

[14] Grimm JB, Brown TA, Tkachuk AN, Lavis LD. General Synthetic Method for Si-Fluoresceins and Si-Rhodamines. ACS Cent Sci 2017;3:975–85. https://doi.org/10.1021/acscentsci.7b00247.

[15] Koide Y, Urano Y, Hanaoka K, Terai T, Nagano T. Evolution of Group 14 Rhodamines as Platforms for Near-Infrared Fluorescence Probes Utilizing Photoinduced Electron Transfer. ACS Chem Biol 2011;6:600–8. https://doi.org/10.1021/cb1002416.

[16] Chai X, Cui X, Wang B, Yang F, Cai Y, Wu Q, et al. Near-Infrared Phosphorus-Substituted Rhodamine with Emission Wavelength above 700 nm for Bioimaging. Chem – Eur J 2015;21:16754–8. https://doi.org/10.1002/chem.201502921.

[17] Fukazawa A, Suda S, Taki M, Yamaguchi E, Grzybowski M, Sato Y, et al. Phospha-fluorescein: a red-emissive fluorescein analogue with high photobleaching resistance. Chem Commun 2016;52:1120–3. https://doi.org/10.1039/C5CC09345G.

[18] Liu J, Sun Y-Q, Zhang H, Shi H, Shi Y, Guo W. Sulfone-Rhodamines: A New Class of Near-Infrared Fluorescent Dyes for Bioimaging. ACS Appl Mater Interfaces 2016;8:22953–62. https://doi.org/10.1021/acsami.6b08338.

[19] Golden JH, Facendola JW, Sylvinson M. R. D, Baez CQ, Djurovich PI, Thompson ME. Boron Dipyridylmethene (DIPYR) Dyes: Shedding Light on Pyridine-Based Chromophores. J Org Chem 2017;82:7215–22. https://doi.org/10.1021/acs.joc.7b00786.

[20] Scheibe G, Friederich HJ, Gückel W, Smits J. Synthese von Chinolinrot-Farbstoffen1. Angew Chem 1961;73:736–736. https://doi.org/10.1002/ange.19610732206.

[21] Friedrich HJ, Gückel W, Scheibe G. Synthesen und Reaktionen der Chinolylmethane, II. Chem Ber 1962;95:1378–87. https://doi.org/10.1002/cber.19620950610.
[22] Tverdiy DO, Chekanov MO, Savitskiy PV, Syniugin AR, Yarmoliuk SM, Fokin AA. Efficient Preparation of Imidazo[1,5-*a*]pyridine-1-carboxylic Acids. Synth Ger 2016;48:4269–77. https://doi.org/10.1055/s-0035-1561489.
[23] Volpi G, Garino C, Priola E, Diana E, Gobetto R, Buscaino R, et al. Facile synthesis of novel blue light and large Stoke shift emitting tetradentate polyazines based on imidazo[1,5-*a*]pyridine – Part 2. Dyes Pigments 2017;143:284–90. https://doi.org/10.1016/j.dyepig.2017.04.034.
[24] Volpi G, Lace B, Garino C, Priola E, Artuso E, Cerreia Vioglio P, et al. New substituted imidazo[1,5-*a*]pyridine and imidazo[5,1-*a*]isoquinoline derivatives and their application in fluorescence cell imaging. Dyes Pigments 2018;157:298–304. https://doi.org/10.1016/j.dyepig.2018.04.037.
[25] Schäfer G, Ahmetovic M, Abele S. Scalable Synthesis of Trifluoromethylated Imidazo-Fused N-Heterocycles Using TFAA and Trifluoroacetamide as CF3-Reagents. Org Lett 2017;19:6578–81. https://doi.org/10.1021/acs.orglett.7b03291.
[26] Amini-Rentsch L, Vanoli E, Richard-Bildstein S, Marti R, Vilé G. A Novel and Efficient Continuous-Flow Route To Prepare Trifluoromethylated N-Fused Heterocycles for Drug Discovery and Pharmaceutical Manufacturing. Ind Eng Chem Res 2019;58:10164–71. https://doi.org/10.1021/acs.iecr.9b01906.
[27] Pidcock E. Achiral molecules in non-centrosymmetric space groups. Chem Commun 2005:3457–9. https://doi.org/10.1039/B505236J.
[28] Ulrich G, Ziessel R, Harriman A. The Chemistry of Fluorescent Bodipy Dyes: Versatility Unsurpassed. Angew Chem Int Ed 2008;47:1184–201. https://doi.org/10.1002/anie.200702070.